JOURNAL OF GEOPHYSICAL RESEARCH, VOL. 113, D09301, doi:10.1029/2007JD009229, 2008

Global AIRS and MOPITT CO measurements: Validation, comparison, and links to biomass burning variations and carbon cycle

Leonid N. Yurganov,[1] W. Wallace McMillan,[1] Anatoly V. Dzhola,[2] Evgeny I. Grechko,[2] Nicholas B. Jones,[3] and Guido R. van der Werf[4]

Received 27 July 2007; revised 14 November 2007; accepted 29 January 2008; published 10 May 2008.

[1] New results of CO global total column measurements using the Atmospheric Infrared Sounder (AIRS) aboard the Aqua satellite in comparison with Measurements of Pollution in the Troposphere (MOPITT) sensor aboard the Terra satellite are presented. Both data sets are validated using ground-based total column measurements in Russia and Australia. A quality parameter based on the *Profile Percent A Priori* values from the standard MOPITT product is introduced. AIRS data (version 4) for biomass burning events are in agreement or lower than both MOPITT and ground measurements, but CO bursts can be seen by AIRS in most cases. For the cases of low CO amounts in the Southern Hemisphere AIRS has a positive bias of ~30–40% compared to MOPITT and ground truth. MOPITT data were used to estimate interannual variations of CO sources assuming a standard seasonal cycle for the main CO remover OH. A positive trend of CO global emissions for the second half of the year between 2000 and 2006 was found with no visible trend for the first half of the year. CO annual emission in 2006 was 184 ± 40 Tg higher that that in 2000–2001. The monthly emission anomalies correlate well with an independently calculated Global Fire Emission Database (GFED2). Total carbon contribution from biomass burning in 1997, 1998 (both estimated by GFED2), and 2006 (according to MOPITT) were as high as (0.6–1) Pg C/year larger than in 2000, suggesting that fires can explain a substantial fraction of the interannual variability of CO_2.

Citation: Yurganov, L. N., W. W. McMillan, A. V. Dzhola, E. I. Grechko, N. B. Jones, and G. R. van der Werf (2008), Global AIRS and MOPITT CO measurements: Validation, comparison, and links to biomass burning variations and carbon cycle, *J. Geophys. Res.*, *113*, D09301, doi:10.1029/2007JD009229.

1. Introduction

[2] Climate change caused by increasing concentrations of greenhouse gases is currently at the center of both scientific and general discussions. Carbon dioxide and methane, according to the fourth assessment report (AR4) of the Intergovernmental Panel on Climate Change (IPCC) [*Solomon et al.*, 2007], contribute 1.66 and 0.48 W $m^{-2,}$ respectively, to the total 2.94 W m^{-2} anthropogenic global mean radiative forcing due to gases (i.e., 73% together). Emissions of these gases from the combustion of fossil fuel and other processes under direct human control can be calculated with high accuracy. Conversely, calculations of emissions from wild fires remain uncertain due to problems with emission factors, available carbon, and imprecise estimates of burned areas. Meanwhile, an intensification of wild fires with climate change potentially provides a positive feedback mechanism, as the frequency and intensity of droughts in continental areas are predicted to increase [*Cox et al.*, 2000, *Solomon et al.*, 2007]. It should be noted, however, that within boreal forests, multidecadal increases in surface albedo may have a climate impact comparable to fire-emitted greenhouse gases, thus canceling some of the warming at a regional scale [*Randerson et al.*, 2006]. The frequency of lightning, the main natural cause of forest fires, is also found to increase with air temperature by ~10% per degree [*Williams*, 1992, 1994; *Price*, 1993]. Finally, an intensification of industrial and agricultural activities in forested areas could result in a growth of biomass burning. Together, all these issues call for reliable experimental techniques for monitoring global and regional emissions from biomass burning.

[3] It is well known that the main areas of wild biomass burning lie in the tropical and subtropical areas of Africa, South America, South-East Asia, Indonesia, and Australia, as well as the boreal forests of North America and Asia [*van der Werf et al.*, 2006]. However, these areas are often

[1]Joint Center for Earth System Technology, University of Maryland, Baltimore County, Baltimore, Maryland, USA.
[2]Obukhov Institute of Atmospheric Physics, Russian Academy of Sciences, Moscow, Russia.
[3]Department of Chemistry, University of Wollongong, Wollongong, New South Wales, Australia.
[4]Department of Hydrology and Geo-Environmental Sciences, Vrije Universiteit, Amsterdam, Netherlands.

0148-0227/08/2007JD009229$09.00

sparsely populated and mostly located far from ground-based observational networks.

[4] Satellite-borne instruments, capable of measuring the tropospheric composition, provide an opportunity for global monitoring of these emissions. Global distributions of CO_2 and CH_4 were measured by Scanning Imaging Absorption Spectrometer for Atmospheric Chartography (SCIAMACHY) [*Buchwitz et al*., 2005a, 2005b; *Frankenberg et al.*, 2006]. Atmospheric Infrared Sounder (AIRS) is capable to monitor these gases as well [*Chahine et al.*, 2005; *Xiong et al.*, 2008]. Unfortunately, the techniques used by these researchers revealed several problems connected with the necessity of very precise measurements ($\sim$1% or better) for these gases, interference from other atmospheric components, insufficient knowledge of temperature profiles, poorly determined vertical sensitivity functions, etc. The Orbital Carbon Observatory (OCO) that is planned for launch in 2008 [*Crisp et al.*, 2004] is specially designed for CO_2 and is expected to secure the required precision [*Miller et al.*, 2007]. The Greenhouse Gases Observing Satellite (GOSAT), a satellite to monitor the carbon dioxide and the methane globally from orbit [*Hamazaki et al.*, 2005] is scheduled for launch in 2008. Both will measure spectra of near infrared solar radiation reflected from the surface.

[5] The impact of biomass burning on carbon monoxide is easier to measure. The signal from biomass burning amounts to 100% or more of its background. CO has strong absorption lines in the middle IR spectral region that overlap only moderately with water vapor lines. Biomass burning CO emissions amount to 500–700 Tg/a, or $\sim$25% of the global CO budget, according to inverse model results by *Bergamaschi et al.* [2000]. Emissions exhibit large interannual variations (IAV), from 337 to 591 Tg/a, according to an inventory by *van der Werf et al.* [2006]. The main other CO sources, incomplete combustion of fossil fuel, chemical conversion from methane, and nonmethane hydrocarbons (NMHC), do not show as much IAV [*Bergamaschi et al.*, 2000]. CO contributes only weakly to greenhouse warming because its fundamental vibration-rotation band near 4.63 μm lies far from the spectral maximum of the Earth's outgoing radiation ($\sim$8–10 μm). Nevertheless, increases in CO can increase the lifetime of atmospheric methane by consuming OH [*Butler et al.*, 2005]. Measurements of CO IAV also enable monitoring of the intensity of biomass burning and indirectly the emissions of carbon dioxide and methane (i.e., total carbon).

[6] Until 2000 quasi-global measurements of CO mixing ratio in the Planetary Boundary Layer were conducted at the ground-based NOAA network and emissions from 1997 to 1998 wild fires were analyzed [*Novelli et al.*, 2003]. Later on estimates of emissions from Siberian fires of 1998 using both surface and total column spectroscopic measurements were derived [*Yurganov et al.*, 2004].

[7] For the first time tropospheric CO was measured from space by the MAPS (Measurements of Atmospheric Pollution from Space) instrument during three flights of the Space Shuttle [*Reichle et al.*, 1999]. The first operational space-borne instrument measuring tropospheric MOPITT [*Drummond*, 1992], provides valuable information about the global distribution of CO with the nominal precision ± 10%. Several papers based on MOPITT measurements, devoted to biomass burning emissions, have been published [*Edwards et al.*, 2004, 2006, and references therein]. *Edwards et al.* [2004] found that the winter and spring of 2002–2003 showed anomalously high Northern Hemisphere (NH) pollution compared to the previous years. This was a result of fires in western Russia in the late summer and fall of 2002 and intense fires in southeastern Russia in the spring and summer of 2003. According to *Edwards et al.* [2006], an annual austral springtime peak in the South Hemisphere (SH) zonal CO loading each year coincides with dry season biomass burning emissions in South America, southern Africa, the maritime continent (Indonesia and surrounding countries), and northwestern Australia. The most significant interannual variation at the maritime continent and northern Australia correlates well with the El Nino–Southern Oscillation precipitation index.

[8] A common problem when converting the measured CO total column or spatially averaged concentration into an emission rate is dealing with rapid mixing by atmospheric winds and convection [*Pétron et al.*, 2004]. In the northern midlatitudes, for example, a predominant circumpolar flow mixes North American and Asian air within several weeks [*Damoah et al.*, 2004] and the analysis requires very sophisticated three-dimensional (3-D) global or hemispheric models to take this transport into account [*Pfister et al.*, 2005]. In addition, the problem of vertical air motion connected with pyroconvection complicates modeling [*Leung et al.*, 2007]. A global one-box model used in this paper allows one to avoid these problems.

[9] Most of the ground-based MOPITT validation experiments (e.g., by *Emmons et al.* [2004, 2007]) were carried out in areas without strong surface emissions. Also, measurements in continental areas over frozen underlying surface have not been validated properly. A low sensitivity of MOPITT to the boundary layer is a limiting factor for measurements of biomass burning products if they are concentrated near the surface [*Deeter et al.*, 2004]. The present paper reports results of concurrent ground-based spectroscopic measurements of CO total column amounts over two locations in the Northern and Southern Hemisphere and comparisons with two space-borne instruments, MOPITT and AIRS. Our intention for the future is to reconcile MOPITT CO data with improved versions of the data from space-borne instruments (AIRS, TES, IASI, SCIAMACHY, etc.).

[10] Another objective is to use the CO emissions as a proxy for CO_2 and CH_4 biomass burning emissions. The emission ratios of total C to CO vary across a wide range and strongly depend on burning conditions and type of biome (examples are given in Table 1). Nevertheless, emission estimates based on potential direct satellite CO_2 and CH_4 measurements would be even less precise and, anyway, require independent sources of information.

2. Experimental

[11] The satellite-borne MOPITT instrument is a part of the Terra platform launched in December 1999. It is a thermal IR nadir-viewing gas correlation radiometer described in detail by *Drummond* [1992] and *Deeter et al.* [2003]. MOPITT uses a cross-track scan with a swath of 700 km, which allows for almost complete coverage of the Earth's surface in about 3 d, with individual pixels of

Table 1. Emission Factors (EF) for Different Biomes[a]

Biome	EF, CO	EF, C	C/CO
Savanna	65	450	6.9
Tropical forest	104	450	4.3
Extratropical forest	107	450	4.2
Peat	200	450	2.3

[a]Emission factors are measured in grams of gas per kilograms of dry matter [*Andreae and Merlet*, 2001]. Carbon content of the dry matter is assumed to be 450 g per kilogram (45%) [*van der Werf et al.*, 2006]. Last column is ratio g C/g CO.

22 km × 22 km horizontal resolution. The sensitivity of the instrument significantly decreases in the boundary layer [*Deeter et al.*, 2004]. The measured total column, therefore, depends on an a priori profile. The data are publicly available at ftp://l0dps01u.ecs.nasa.gov/.

[12] Launched on board NASA's Aqua satellite on 4 May 2002, the AIRS cross-track scanning grating spectrometer provides vertical profiles of the atmosphere with a nadir 45 km field-of-regard across a 1650 km swath [*Aumann et al.*, 2003; *Chahine et al.*, 2006]. Although primarily designed as a prototype next generation temperature and water vapor sounder, the broad spectral coverage of AIRS (3.7 to 16 μm with 2378 channels) includes spectral features of O_3, CO_2, CH_4, and CO [*Haskins and Kaplan*, 1992]. With such a broad swath, AIRS infrared spectra and cloud-clearing [*Susskind et al.*, 2003] enable day/night retrievals over nearly 70% of the planet every day (100% daily coverage between 45° and 80° latitude in both hemispheres), with substantial portions of the globe observed twice per day (ascending and descending orbits). Thus, AIRS readily observes global scale transport from large biomass burning sources [*McMillan et al.*, 2005]. The AIRS mixing ratios for the 500 mb level between 15 June and 14 August 2004 were validated by *Warner et al.* [2007]. Satellite data agree with airborne measurements to within an average of 10–15 ppbv. The data version 4.2, used by *Warner et al.* [2007], however, was different from that used in the present paper. The AIRS spectra are reprocessed now and the versions 4 and 5 are available at (http://disc.gsfc.nasa.gov/AIRS/index.shtml).

[13] Ground-based total column validation data in the NH were obtained from the Zvenigorod Research Station affiliated with the Institute of Atmospheric Physics (IAP), Russian Academy of Sciences, near Moscow (55.70°N, 36.78°E, 198 m above sea level). A sun tracking Ebert/Fastie-type grating spectrometer with 855 mm focal length and a grating of 300 grooves/mm was employed for measuring absorption spectra of the atmosphere. The instrument was designed and constructed at the IAP [*Dianov-Klokov*, 1984]. It has a resolution of approximately 0.2 cm^{-1} in the 2152–2160 cm^{-1} spectral region, with a signal-to-noise ratio better than 100 and is equipped with a thermoelectrically cooled PbSe detector. Detectors of this type and corresponding spectral resolution have been used since 1974. The retrieval code is written in MATLAB and uses standard nonlinear least squares procedures provided by MATLAB [*Mc Kernan et al.*, 1999]. A priori profile of CO concentration (the same as that used in MOPITT retrievals: 120 ppb near the surface and decreasing mixing ratio with height down to 80 ppb just below the tropopause) was iteratively scaled to minimize the residual between measured and calculated spectra. Insufficient spectral resolution does not allow for retrieval of CO profiles from this instrument. CO total column amount is measured with typical estimated uncertainty for an individual measurement of 7–8% [*Yurganov et al.*, 2002]. The maximum error can be expected for days with an extremely polluted boundary layer; e.g., special calculation using an a priori profile with 4 ppm mixing ratio near the surface reduces the CO column by 17% compared to the standard a priori. In Zvenigorod, these conditions happen very rarely. Such a case of strong pollution from peat fires in September 2002 was analyzed by *Edwards et al.* [2004].

[14] Regular measurements of CO total column in Zvenigorod started in 1971. CO seasonal variations with a maximum in March–April and a minimum in August were found in the late 1970s [*Dianov-Klokov and Yurganov*, 1981]. Between 1970 and 1985, CO increased; after 1985 no significant long-term trend was observed until 1996 [*Yurganov et al.*, 2002]. Interannual variations of CO during this period were explained partly by major volcanic eruptions and partly by biomass burning [*Yurganov et al.*, 1997]. During the most recent period, the CO total amount seemed to decline (with the exceptions of the forest-fire-impacted years 1998, 2002, and 2003) [*Yurganov et al.*, 2002, 2005].

[15] A complementary observatory, affiliated with the Network for Detection of Atmospheric Composition Change (NDACC), at Wollongong, New South Wales, southeast Australia (50 km from Sydney, 34.45°S, 150.88°E, 20 m above sea level) provided ground truth validation data for the SH. Extensive investigations of biomass gaseous products were carried out using Fourier Transform Infrared Spectrometer (FTIR) [*Paton-Walsh et al.*, 2005]. Between April 2000 and December 2006, infrared solar atmospheric absorption spectra were recorded using a Bomem DA8 high-resolution Fourier transform infrared spectrometer coupled to a solar tracker. Typical measurement times per spectrum ranged from 3 to 15 min depending on the optical path difference employed (50 to 250 cm); the mean total number of spectra per day was 3 and varied from 1 to 6. The number of CO molecules per square centimeter above the measurement site (the vertical column amount) was derived from individual spectra by iteratively adjusting the concentration of CO in simulated spectral intervals until the difference between measured and simulated spectra was minimized. The simulated spectrum used a layered model of the atmosphere, with the pressure, temperature, and an initial concentration for CO assigned over 39 layers. Retrievals were performed using the SFIT2 nonlinear iterative fitting algorithm [*Rinsland et al.*, 1998], which is based on the Rodgers optimal estimation method [*Rodgers*, 2000] returning the concentration profile of the target gas which best fits a suitably weighted combination of the measured and simulated spectra. The a priori profile of the simulated spectrum is weighted by the covariance matrix, a matrix that defines the expected variation in the concentration of the target gas at each layer of the simulation. The 39 individual layers in the forward model of the simulated spectrum are by no means independent. The estimated number of independent points in the profile is between 3 and 4, depending on a range of factors that include the assumed measurement noise and solar zenith angle. The total uncertainty of the CO total column amounts

is estimated as 6.5% [*Paton-Walsh et al.*, 2005] and typical standard deviations of individual retrievals were between ±2 and ±6%. The altitude sensitivity functions for both instruments (the Fourier Transform and grating spectrometers) maximize near the surface and gradually decrease throughout the troposphere; the decline of sensitivity for the Zvenigorod grating instrument is larger due to lower spectral resolution.

3. Validation and Biomass Burning Local Events

3.1. Ground-Based Validation

[16] Both satellite- and ground-based instruments measure CO total column amounts in molecules/cm^2. However, the vertical sensitivities of the different instruments are altitude dependent and, as a result, the measured values depend on (1) the a priori profile used in the forward model, (2) the actual CO vertical distribution, and (3) the averaging kernel as a function of altitude (being equal to 1.0 for ideal vertical sensitivity) [*Rodgers*, 2000]. If the actual CO profile is close to the a priori, then a virtual agreement for instruments with nonidentical averaging kernels cannot be excluded. Otherwise, in an unusual case (e.g., for strong surface emissions and a polluted boundary layer) more significant differences can be found.

[17] Ground-based validation sites, selected in this study, represent midlatitude Northern and Southern Hemispheric locations subjected to biomass burning pollution in spring, summer, and autumn seasons of the year. In addition, the northern site gives a unique chance to verify MOPITT data measured over a frozen underlying surface in the winter time, when lower thermal contrast between the surface and the atmosphere is expected to drop its accuracy [*Deeter et al.*, 2003].

[18] The NH validation site, Zvenigorod, may be affected by local and/or remote biomass burning emissions during spring, summer, and fall. In winter, the surface is normally snow covered and air temperatures are below the freezing point. An example of MOPITT, AIRS, and ground-based data for all of 2006 is plotted in Figure 1a. CO total column amounts were measured in Zvenigorod generally between 0900 and 1400 local Moscow time, with 10–25 spectra per day recorded and standard deviation (STD) of individual retrievals ±(2–5)%. For both satellites, we used daily gridded satellite data (averaged over 1° × 1°) centered at 55.5°N, 36.5°E. Owing to a wider swath, the number of Zvenigorod points for AIRS is much higher than that for MOPITT. The numbers of individual retrievals for matching days were from 1 to 15 for MOPITT and from 1 to 8 for AIRS. Typical STD for MOPITT data were around ±5% in daytime and ±(15–20)% in nighttime, both in summer. In winter STD increased up to ±30% for all data. STDs for AIRS were normally between ±2 and ±5%. For periods of biomass burning STDs increase up to ±(15–25)% and in these cases the scatter represents spatial variations in biomass burning plumes. The maximum distance between individual satellite data points and Zvenigorod was around 100 km and the square area corresponding to satellite data did not cover the city of Moscow.

[19] Periods of agreement and disagreement between satellites and Sun-viewing spectrometers can be noted in Figure 1. This comparison may help in determining a quality parameter for satellite data. A parameter *CO Profile Percent A Priori (PPA)* is specified for every data point and every pressure level in the standard MOPITT product. For each level in the profile, PPA is just the ratio of the corresponding diagonal elements of the retrieved error covariance matrix and the a priori covariance matrix. As this value approaches 100%, the uncertainty in the retrieval is the same as the a priori uncertainty, and therefore no information from the observations has been added. As this value approaches 0, the retrieved value is almost exact (M. Deeter, personal communication, 2007). Daily means of PPA for the Zvenigorod grid cell and for the whole period of measurements for two layers are plotted in Figure 2. The top panel is for daytime; the bottom one is for nighttime data. Reported total columns are essentially a result of the integration of CO profiles and no quality parameters are available in the standard product. In this paper we define a Total Column Quality Parameter (TCQP), calculated as the pressure-weighted mean of PPA over six levels between 1000 and 250 mb, indicated by blue triangles and stars in Figure 2. PPA experiences seasonal cycles both for the surface layer (1000 mb) and for the free troposphere (500 mb) during both daytime and nighttime. At nighttime (red squares, bottom panel), MOPITT appears practically insensitive to the boundary layer year-round, in contrast to a better sensitivity during the daytime (red circles, top panel). Winter is generally the worst season for all MOPITT data; however, on some days the PPA at 500 mb drops to 20–30%. TCQP has typical values of 30% during day and 45% during summer nights. It increases toward the cold season. The aim of this validation effort is to determine a universal threshold for the TCQP that can be used in data filtering.

[20] At Zvenigorod, relatively good agreement for all data is noteworthy for the period between April and September (days 90–270; Figure 1a). Two biomass burning events were identified using the Along Track Scanning Radiometer (ATSR) nighttime fire counts (http://dup.esrin.esa.int/ionia/wfa/index.asp, described by *Arino and Plummer* [2001]). The ATSR instrument detected fires in the area [50°N–60°N, 30°E–42°E] between days 100 and 140. Strong regional biomass burning occurred in April to May in the central part of European Russia and the Baltic countries, Ukraine and Belarus (North of 40°N and between 20° and 60°E). According to *Stohl et al.* [2007], more than 300 fires/d were detected by MODIS in this area from 25 April (day 115) to 6 May 2006 (day 126), with a peak of more than 800 detections on 2 May (day 122). This led to an estimate of almost 2 million hectares burned in April and May 2006. This emitted CO and smoke were transported to the Arctic and observed at Spitsbergen and by AIRS [*Stohl et al.*, 2007]. These experimental data were in agreement with calculations by the 3D FLEXPART model [*Stohl et al.*, 2005]. During the daytime, enhanced CO values were clearly detected over Zvenigorod by MOPITT. CO columns measured by AIRS generally were lower than MOPITT but higher than normal values at the end of May (after day 140) when the fires stopped. Maximum CO columns around (3.5–3.7) × 10^{18} molecules/cm^2 were measured both by MOPITT and by the Sun-viewing spectrometer.

[21] Some fires and small variations of CO column were detected near Zvenigorod in July to August (days 180–240). An extremely high CO column amount was mea-

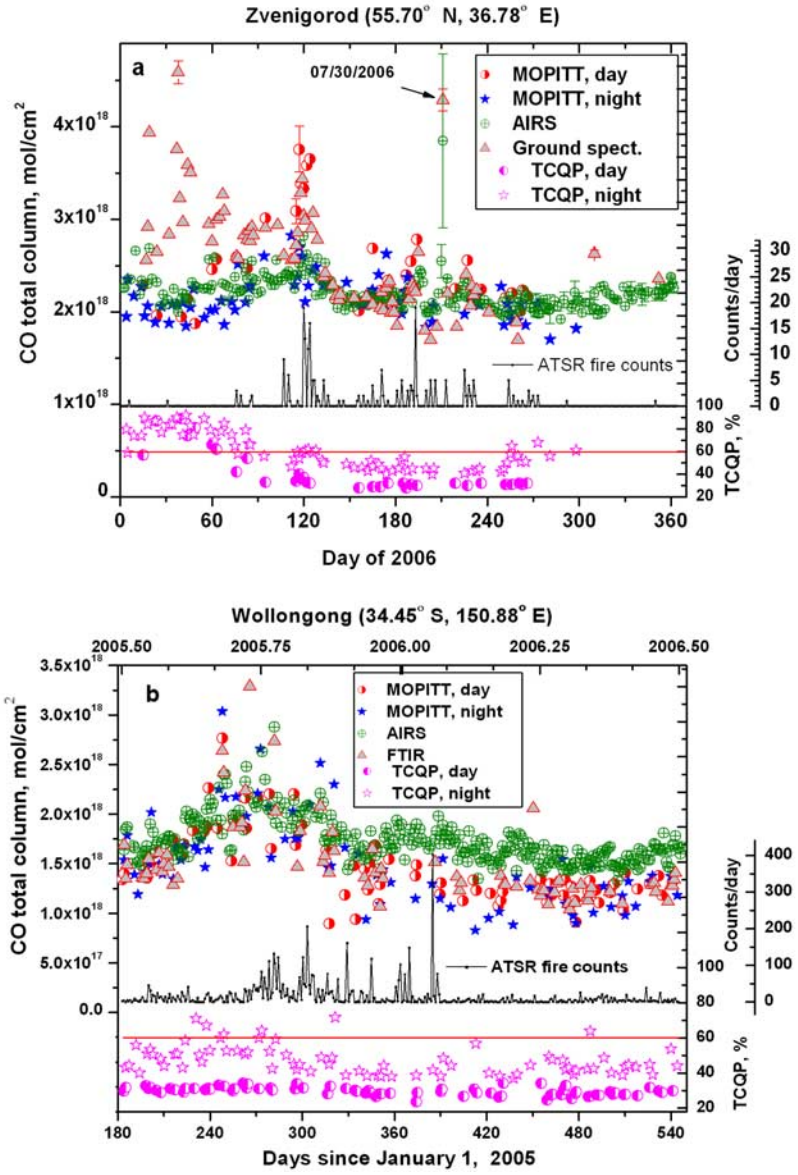

Figure 1. (a) Daily mean CO total column amounts averaged for the area [55.0°N–56.0°N, 36.0°E–37.0°E] for AIRS and MOPITT data sets; for MOPITT daytime and nighttime data are plotted separately. Ground-based grating spectrometer data are used as ground truth. STDs are shown by vertical bars; in cases of no error bars STD coincided with the size of symbols. ATSR fire counts are summed daily for the area 49°N–61°N, 30°E–42°E. Total column quality parameter (TCQP) for MOPITT data is derived from profile percent a priori values (see text). (b) The same as Figure 1a, but for the area [34.0°S–35.0°S, 150.0°E–151.0°E]. FTIR spectrometer data are used as a ground truth. ATSR fire counts are summed for the area [49°S–61°S, 30°E–42°E].

sured both by ground-based spectrometer (19 spectra) and AIRS (5 spectra) on 30 July 2006 (day 211). Interestingly, no significant fires were detected during this or adjacent days. The difference between the two measurements was just 11% with daily mean column amounts more than 4×10^{18} molecules/cm^2. The unusually large scatter of AIRS individual retrievals reflects horizontal inhomogeneity of the CO field. The closest AIRS retrieval to Zvenigorod on 30 July 2006 is only 1.2% larger than the ground-based measurement. MOPITT data were not available for this area and this day. According to analysis of the CO and Ozone Monitoring Instrument (OMI) aerosol index maps for previous days, on 30 July the area of Zvenigorod was impacted by a plume from forest fires that occurred in central Siberia (around 57°N, 95°E) between 18 July and 24 July 2006 (a movie file is available online at ftp://fennel.umbc.edu/incoming/yurganov/CO_aerosol_2006.ppt). This plume split into roughly equal halves on 25 July, with one half moving to the northwest, then to the southwest reaching Zvenigorod on 30 July. The other half of the plume moved to the east and reached Alaska by the end of July (see also the analysis of Siberian region below).

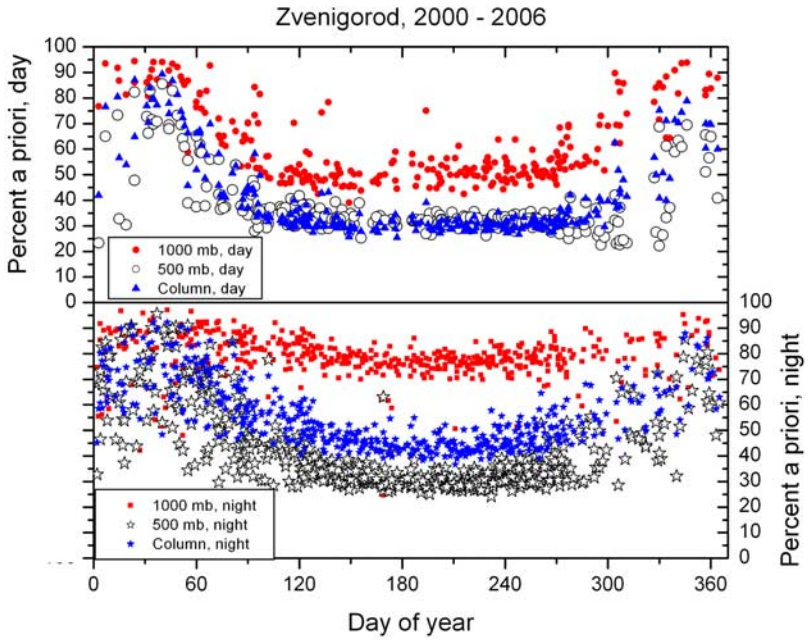

Figure 2. MOPITT 1000 mb and 500 mb CO profile percent a priori (PPA) daily mean values for the Zvenigorod grid cell for the whole period of MOPITT measurements. Blue triangles and stars are pressure weighted averages of PPA over six layers from 1000 mb to 250 mb (TCQP in the text).

[22] TCQP values, plotted in the bottom of Figure 1a, explain the errors in MOPITT data. CO MOPITT measurements with a TCQP around 30–40% agree with ground truth data. For TCQP > 60% MOPITT data, both daytime and nighttime, disagree with ground truth data. As a result, a large disagreement is observed in January to February (days 1–60).

[23] Figure 1b demonstrates an example of the measurements of CO total column amounts in southeast Australia between 1 July 2005 and 30 June 2006. Note that the period shown has been shifted by 0.5 year to reconcile seasons with Figure 1a. Wollongong is located closer to the equator than Zvenigorod and winter surface temperatures, both daytime and nighttime, are higher than for the NH validation site. Good agreement between all MOPITT data and ground truth is observed. During the SH winter-spring time and periods with high CO columns (July 2005 to October 2005), the agreement between AIRS and ground truth is good. However, AIRS data has a positive bias of 30–40% in the SH summer-autumn time, between January 2006 and June 2006.

[24] Figure 3 demonstrates the dependence of MOPITT error (MOPITT CO minus ground truth divided by ground truth) on TCQP. All matching days for the period 2000–2006 were plotted (276 d for Zvenigorod and 262 d for Wollongong). Values of 72% and 81% of MOPITT daily mean values for Zvenigorod and Wollongong, respectively, differ less than 20% from the ground truth. A scatter for individual days is explained partly by an imprecise coincidence in both the space and time of the measurements, as well as experimental errors in ground truth data. The accuracy of MOPITT retrievals apparently decreases for TCQP > 60%. Mean percent errors for Zvenigorod (after filtering out dates with TCQP > 60%) are 4.5 ± 13.3 for daytime; −6.1 ± 15.1 for nighttime. For Wollongong they are 0.7 ± 12.7 for daytime; +1.5 ± 19.0 for nighttime. In this regard, nighttime MOPITT total column data for continental areas like Zvenigorod with TCQP ∼ 40–50% in summertime (Figure 1a) should be considered as less reliable, and wintertime observations with TCQP > 60% as unreliable. These results correlate to validation experiments, conducted during day time with biases in percent: 4.9 ± 10.8 (2000–2001), 0.5 ± 12.1 (2001–2002), 5.4 ± 7.1, 7.7 ± 8.3 (2004) and reported by *Emmons et al.* [2004, 2007].

[25] Of special interest is a question of the long-term temporal stability of the MOPITT instrument itself. All available validation data were averaged yearly and plotted on the same graph (Figure 4; the yearly averages for the four subsets are slightly shifted along the time axis for clarity). Because any instrumental trend in the MOPITT data, if it

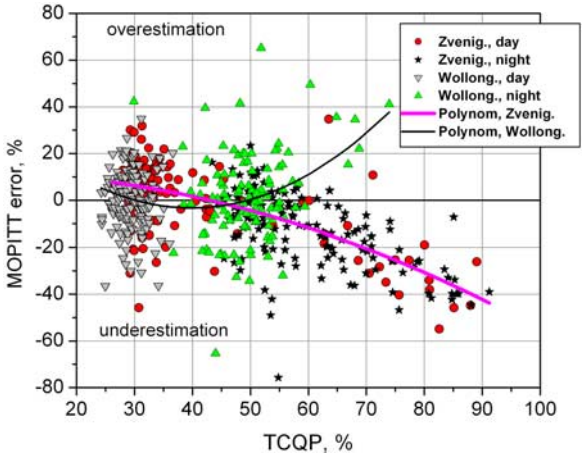

Figure 3. Errors of daily averages of MOPITT data observed during daytime and nighttime for matching days between 2000 and 2006 (MOPITT subtracted by ground truth, divided by ground truth, and multiplied by 100) plotted as a function of the TCQP.

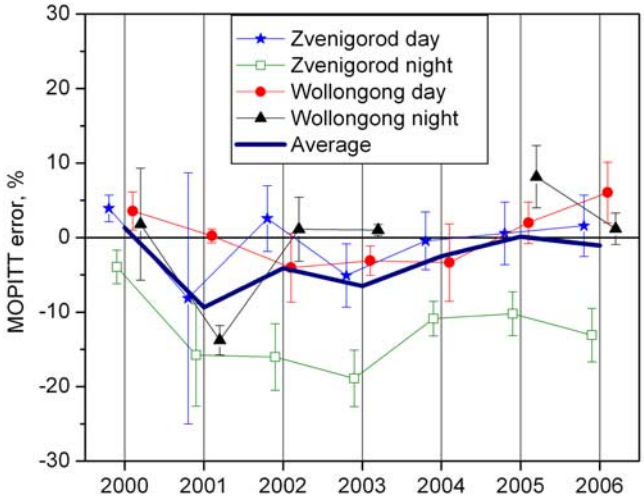

Figure 4. Yearly averaged MOPITT error for the entire validation period and two validation sites.

really exists, should influence all the data, the data were averaged together (Figure 4, thick blue line). A 10% drop occurred from 2000 to 2001, and a positive trend was observed afterward (~8% in 5 years). This drift may be attributed to instrumental and/or retrieval errors. The significant scatter of data on this plot, however, makes this conclusion premature; more long-term validation data are necessary.

3.2. MOPITT Versus AIRS

[26] This section is devoted to comparisons between AIRS (day and night together) and MOPITT (day and night separately) for regional and global cases. The regions with high biomass burning rates in 2006 were selected. Figure 5a demonstrates variations of CO total column daily values in 2006, averaged over Siberia (45°N–69°N, 80°E–180°E) together with ATSR fire counts and MOPITT's TCQP (unfortunately there are no ground truth observations there and in Indonesia). Wintertime data (days 0–90, 330–365) have TCQP > 60% and, apparently, are not correct. During the rest of the year, AIRS and MOPITT data are in general agreement, excluding the period between April and June (days 90–180). The vertical sensitivity of AIRS appears to be similar to that for nighttime MOPITT with TCQP around 60% and above. Daytime MOPITT data have TCQP <60%, i.e., less than the threshold determined above. The CO decline between May and June (days 120–180) reflects the typical NH seasonal pattern driven by [OH] increase in summertime.

[27] For a period of summer forest fires (between 22 July and 2 August 2006) MOPITT detected increased CO during daytime (with TCQP = 33%), just 7% higher than at night (with TCQP = 50%, e.g., still reliable). Sensitivity of AIRS to this event was similar to nighttime MOPITT data.

[28] Another, and obviously stronger burst of CO occurred in September–October 2006 (days 270–320) in Indonesia (Figure 5b, CO is averaged over the area delimited by 8°S–8°N, 95°E–145°E). High-quality MOPITT data (TCQP = 30~35%) revealed a CO increase in September and October with a magnitude ~150% in the maximum (daily MOPITT averages for 2005 are plotted for comparison). AIRS data are close to MOPITT in August to December 2006 (days 210–365) but 30–40% higher in May and July. The maximum excess of CO column over Indonesia above background amounted to 2×10^{18} molecules/cm^2, compared to 0.5×10^{18} molecules/cm^2, observed in July in Siberia, in spite of a factor of 3 fewer ATSR fire counts. Various explanations of this effect may be proposed (uncertain link between fire counts and actual fires, different CO yields per fire, different intensities of removal by winds, etc.).

[29] The four examples (Figures 1a and 1b and Figures 5a and 5b) demonstrate the good sensitivity of MOPITT daytime measurements to tropospheric CO. Nighttime data appear to be less accurate but useful in many cases, especially near the equator. Wintertime midlatitude continental MOPITT data are unreliable. TCQP, introduced in this paper and calculated from standard PPA values, is a useful criterion for filtering out bad data; the points with TCQP > 60% most likely should be used with caution or discarded. The version 4 of AIRS CO data can be used just for qualitative analysis. A disagreement with MOPITT and ground truth for low CO total columns (in the Southern Hemisphere and near the equator) may be partly explained by unrealistic a priori profile used in AIRS, version 4. This is fixed in the version 5.

[30] In a summary plot, CO daily burdens (total CO mass) measured by MOPITT and AIRS in Northern (0–70°N) and Southern Hemispheres (0–70°S) in 2006 are presented in Figure 6 (the top group of curves). CO burdens in both hemispheres have maxima in spring time and minima in late summer to early autumn. This cycle is dominated by seasonal variations of [OH] that is responsible for 84% of CO removal [*Bergamaschi et al.*, 2000]. Differences between nighttime and daytime MOPITT values in NH are probably explained by different contributions of a priori in the MOPITT retrieval (the bottom group of curves). Nonetheless, the semihemispherical burdens satisfy the quality criterion of TCQP <60% and will be used in the following analysis.

4. CO and Total C Emissions Estimated From CO Burdens

[31] CO monthly mean values of burden between 70°S and 70°N calculated from MOPITT daytime and nighttime measurements taken together are plotted by open black triangles in Figure 7. MOPITT data for regions above 70° are unreliable due to lower temperature contrast between the surface and atmosphere. Standard seasonal cycle was calculated for the 24 month period of March 2000 to February 2002. This cycle was repeated in Figure 7 for all years as a red line and full red circles. During every year the total burden exhibits two maxima, in March and April and in October, and two minima, in June and July and in December and January. The maxima coincide with corresponding seasonal maxima in the Northern and Southern hemispheres and can be explained by seasonal changes in the CO sink, a reaction with OH; [OH] depends on solar radiation and has a minimum in winter time in both hemispheres [*Spivakovsky et al.*, 2000]. The magnitude of the October maximum strongly depends on the intensity of fires during dry seasons

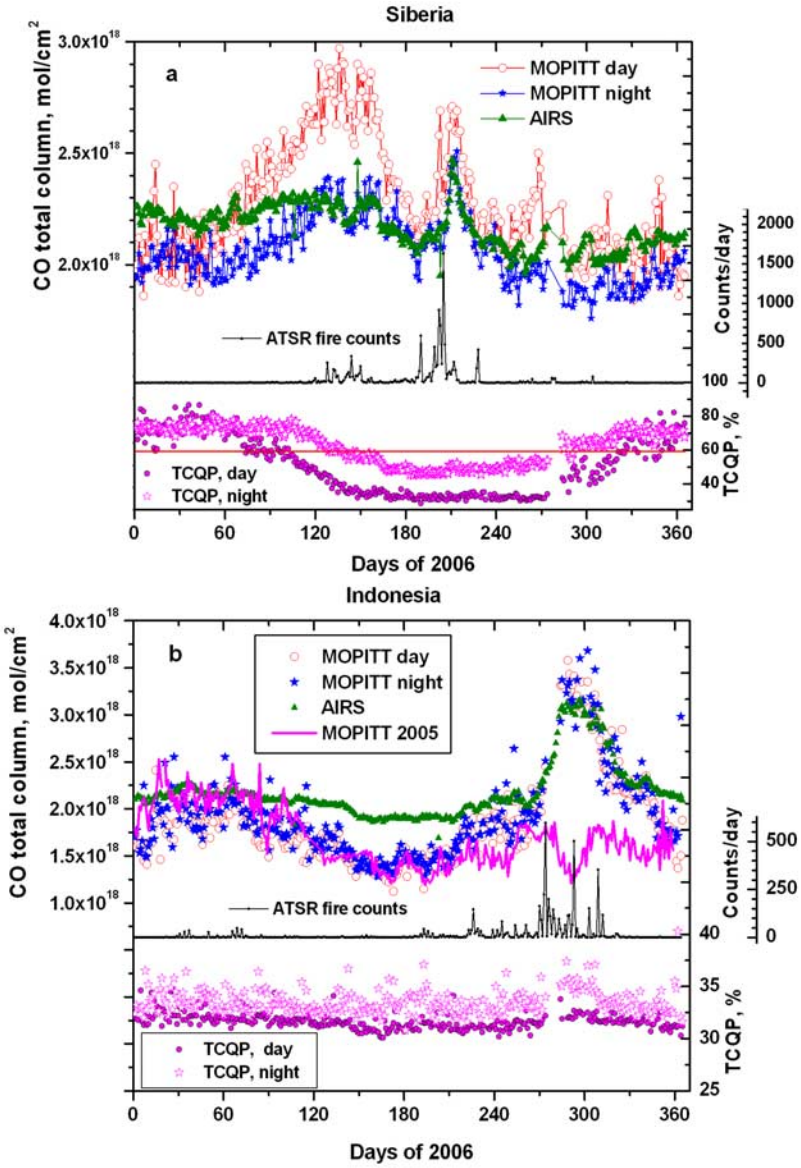

Figure 5. (a) Daily mean CO total column amounts averaged for Siberian area [46.0°N–70.0°N, 80.0°E–180.0°E] for AIRS and MOPITT data sets; for MOPITT daytime and night data are plotted separately. ATSR fire counts are summed daily for the same area. (b) The same as Figure 5a, but for Indonesian area [8.0°S–8.0°N, 95.0°E–145.0°E].

in the tropics taking place between August and November [*van der Werf et al.*, 2006]. The magnitude of the April maximum is less variable because the dominant Northern Hemisphere source, fossil fuel combustion, is relatively constant. For five years starting with 2002, the October seasonal maxima were higher than in 2000, especially in 2002, 2005, and 2006. Mean July to December values were increasing with the rate of +7.5 Tg a^{-1} (1.9% a^{-1}) and R^2 = 0.74. The magnitudes of the April maxima did not differ much from 2000 and 2001. During the first half of the year no significant trend was observed (+1.5 Tg a^{-1} and R^2 = 0.08).

[32] Monthly anomalies of CO burden (differences between black and red curves) are plotted as green squares in Figure 7, middle. An increasing trend of CO burden during the second half of the year is evident.

[33] The monthly anomalies of the CO global emission rate P' (Tg CO/month) were estimated using a box model following *Yurganov et al.* [2004]. The "prime" symbol designates the anomaly, i.e., the deviation from the average over the reference period between March 2000 and February 2002. The box boundaries are at 70°S and 70°N latitude, between air pressure levels 1000 and 200 mb. The formula follows:

$$P' = dM'/dt + L' \tag{1}$$

$$L' = M' \cdot k \cdot [\mathrm{OH}] \tag{2}$$

$$\mathrm{k} = 1.5 \cdot 10^{-13}(1 + 0.6\,p)\mathrm{cm}^3\ \mathrm{molecule}^{-1}\ \mathrm{s}^{-1} \tag{3}$$

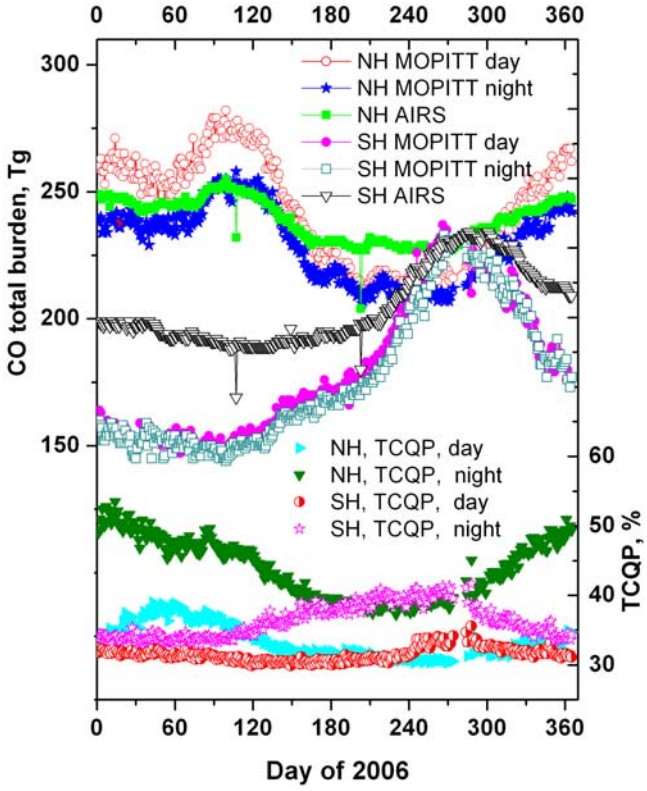

Figure 6. CO daily hemispheric total burdens (mean total column multiplied by the area) for 0°–70°N (NH) and 70°S–0° (SH) measured by two space-borne instruments. Days with TCQP >60% have been filtered out.

[34] [*DeMore et al.*, 1997], where M' is the monthly mean anomaly of CO burden; dM'/dt is the monthly changes of M'; L' is the loss term due to OH-consumption in the troposphere, responsible for 84% of CO removal; 10% are removed by soil bacteria, 6% is consumed by stratospheric OH [*Bergamaschi et al.*, 2000]. [OH] is the hydroxyl concentration; k is the CO + OH reaction rate constant; and p is the atmospheric pressure in atm.

[35] *Yurganov et al.* [2004] estimated uncertainty of the P' for high NH (30°N–90°N) as ±(20–40)%. These estimates included a possible ±50% variation of [OH] and reasonable deviations in CO transport between middle and low latitudes of the NH. The transport term is insignificant for the global case; modern estimates of [OH] variations are much lower than ±50%. Therefore, in this paper the uncertainty of P' may be taken as ±20% (assuming that original MOPITT data are correct).

[36] L' was calculated according to (2) and (3) with the [OH] global seasonal/latitudinal/vertical field, given by *Spivakovsky et al.* [2000] and assumed to be the same for all years. Here L' was calculated for each 1° × 1° grid cell and each month separately and integrated between 70°S and 70°N, 180°W–180°E. Vertical pressure stratification was taken according to 1976 U.S. Standard Atmosphere [*Minzner*, 1977].

[37] The bottom part of Figure 7 illustrates monthly values of dM'/dt, the loss term L', and emission anomalies P' as a function of time. The globally averaged chemical lifetime of CO is approximately 2 months, and the sink term (blue triangles) is important for the calculation of P′.

[38] The red line with open circles represents the "quasi-global" anomalies of CO total emission derived from MOPITT measurements. "Quasi-global" means that beyond 70° latitude there are no significant sources of CO; the chemical removal is slow as well. This P′ can be compared with independently estimated anomalies of emission from biomass burning (GFED2, *van der Werf et al.* [2006], updated for 2006) included in Figure 8 and Figure 9 ("bottom-up" estimates). These two independent estimates correlate both in timing and magnitudes of monthly averages. The squared correlation coefficient is 0.40 and the slope is 0.88 (Figure 9). To illustrate interannual variations of emissions, the monthly data were summed for two halves of the years separately (bottom part of Figure 8). CO emission anomalies during the second half of the year were increasing with time and reached 184 Tg per 6 months in 2006. This is close to the GFED2 estimate for the record year of 1997, dominated by emissions from Indonesian fires of September and October 1997. GFED2 estimates for 2002–2006 are 30–60 Tg lower than corresponding MOPITT estimates.

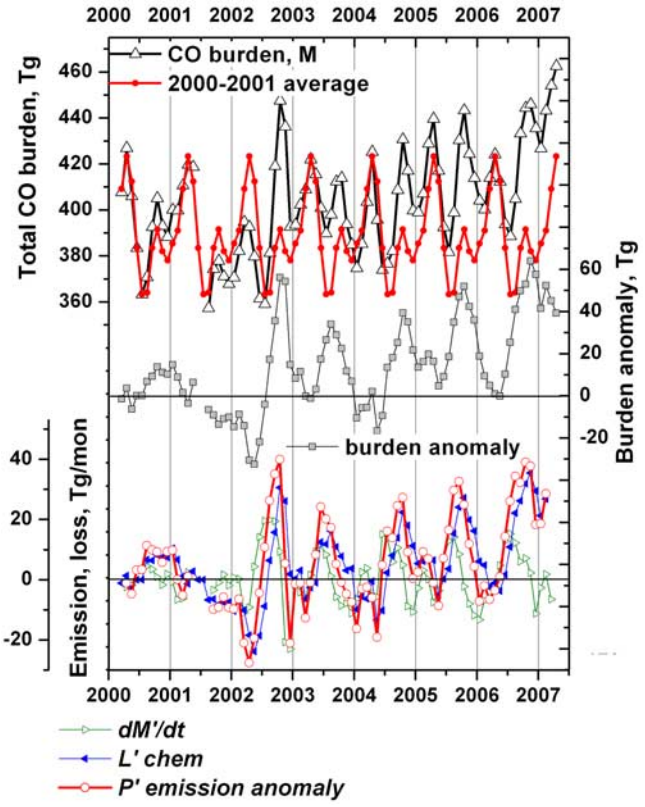

Figure 7. Monthly mean CO burden M (total mass) between 70°S and 70°N measured by MOPITT since March 2000. The period between March 2000 and February 2002 is used as a reference seasonal cycle (red line and dots). The burden anomaly is a difference between measured burden and the reference seasonal cycle. Global (70°S–70°N) CO emission anomaly (red line and open circles) was derived from monthly changes of the burden (green triangles) and chemical removal (blue triangles).

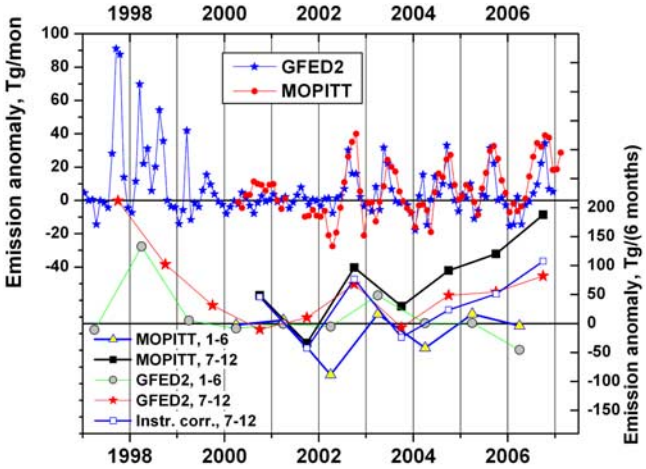

Figure 8. A comparison between CO emission anomalies derived from MOPITT measurements and inventory GFED2 [*van der Werf et al.*, 2006]. (top) Monthly averages and (bottom) semiannual sums, where "1–6" and "7–12" denote periods of averaging in months of the year. "Instr. corr" line is calculated for MOPITT data corrected for the drift (divided by (1+ error) values, plotted in Figure 4, "average" line).

[39] Is this trend a result of the instrumental drift with the magnitude ~+1%/a implied by our validation experiment, as seen in Figure 4? To investigate this possibility we introduced a correction factor based on the average curve from Figure 4 to the measured CO burden and recalculated CO emission anomalies (Figure 8, blue line and open squares). These corrected values agree with GFED2 much better. However, additional verifications of the instrumental trend are necessary.

[40] The sink term L′ is proportional to the burden anomaly M′ and [OH] (equation (2)). *Wang et al.* [2008] estimated mean global [OH] as 9% less than data by *Spivakovsky et al.* [2000]. They used methyl chloroform measurements and three-dimensional global chemistry/transport model. This correction together with removing

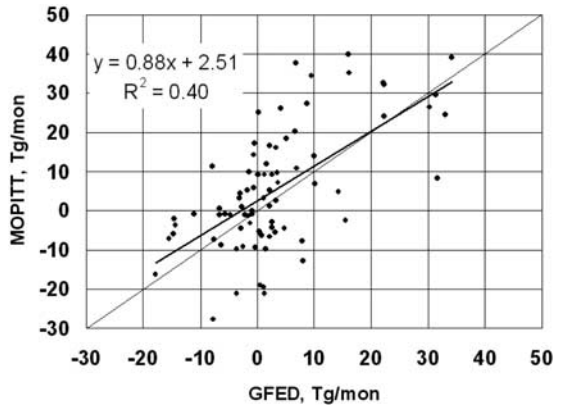

Figure 9. Correlation between CO global emission monthly anomalies, measured by MOPITT and anomalies of CO emission from biomass burning calculated using GFED2 model [*van der Werf et al.*, 2006].

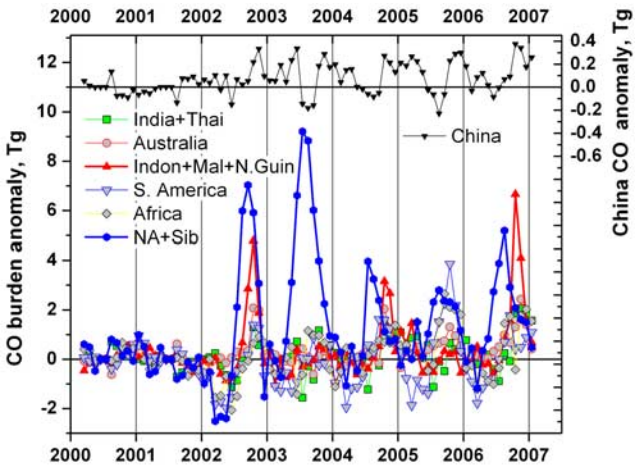

Figure 10. Monthly anomalies (referenced to mean 03/2000–02/2002 values) of CO burden over selected areas on the globe (for boundaries see Table 2). North American and Siberian boreal areas are taken together because of fast circumpolar transport of CO.

instrumental drift probably can resolve the discrepancy between two estimates.

[41] Biomass burning CO emission may not be the only unstable CO source. Some pyrogenic nonmethane hydrocarbons (NMHC), especially isoprene and terpenes, are quickly oxidized to CO. How large is the source of CO from oxidation of pyrogenic NMHC? *Yurganov et al.* [2004] estimated this source as contributing up to 11% of the CO directly emitted during fires. *Van der Werf et al.* [2006] calculated the emission of NMHC as 6.3% of CO using emission factors from *Andreae and Merlet* [2001]; the oxidation of these NMHC would increase the CO source from fires by 9.5%.

[42] Oxidation of NMHC emitted by plants as byproducts of their life cycle contributes ~500 Tg CO/a [*Bergamaschi et al.*, 2000]. *Tao and Jain* [2005] gave model estimates of their IAV ± (17–25)%. *Palmer et al.* [2006] estimated ±40% from formaldehyde satellite measurements over the southeastern United States. Thus, CO variations from oxidation of NMHC would be in the range from 85 to 200 Tg/a. IAV of CO sources from biogenic NMHC require further analysis.

[43] Increasing combustion of fossil fuel may increase CO burden as well. This increase, however, may be expected during the whole year and do not have significant IAV. Nevertheless, to examine this possibility, the CO burden anomaly over China measured by MOPITT was plotted in Figure 10 (black triangles on the top, note different scales for China and other regions). Variations observed over China were less than 1/10 variations in areas with biomass burning.

[44] One can state that according to MOPITT data, global CO emissions have been increasing since the launch of Terra and have now reached 100–200 Tg higher values than in 2000–2001; most (if not all) of this effect should be assigned to the second part of the year. Biomass burning during dry seasons in the tropics and subtropics is the most likely process responsible for this change, although northern midlatitude boreal forest fires, which usually occur in July

Table 2. Boundaries of Areas Selected for Analysis and Corresponding Annual Mean CO Burdens for the Standard Period 03/2000–02/2002

Area	Range of Latitude		Range of Longitude		CO Burden, Tg
India+Thailand	10	30	70	110	8.49
Australia	−40	−15	115	155	7.18
Indones.+Malaisia.+N.Guinea	−10	5	95	145	6.39
China	25	40	105	120	2.25
South America	−40	15	−80	−35	5.98
Africa	−35	15	−20	40	21.11
North America	50	70	−170	−60	12.38
Siberia	46	70	40	170	19.18

and August, contribute as well. Further measurements are necessary to determine is this a cyclic process or a long-term climate trend.

[45] A box model does not allow one to determine the spatial distribution of the emission anomaly. However, contributions from different areas may be qualitatively assessed from measured CO total columns over specific areas. Figure 10 demonstrates regional changes in CO excess monthly mean burden in Tg for selected areas in comparison to the standard period of 2000–2001 (area boundaries and biannual mean burdens for the standard period are presented in Table 2). One should remember that emission anomalies are NOT proportional to the burden anomalies; in midlatitudes the emitted CO lives in the atmosphere 2 or 3 times longer than in the tropics where it is more quickly removed by OH. However, we may conclude that leading roles in the observed emission changes are played by northern boreal fires and Indonesia, while Africa demonstrates a small increasing trend, and South American fires were stronger in 2005. Generally, both Africa and South America contribute less to IAV than Indonesia. Meanwhile, according to *van der Werf et al.* [2006], African biomass burning dominates in total emissions (49%) with South America being the second highest (13%). A smaller, but notable increase of CO burden is observed in SE Asia as well (India and Thailand). Most of these small increases, however, may be attributed to the instrumental drift.

[46] While CO is a good indicator of biomass burning, the importance of this global phenomenon to global change is determined mainly by the emissions of carbon dioxide and, to a less extent, methane. A ratio between CO and total carbon emitted from biomass burning is a function of fuel type, intensity, and the character of a specific fire (Table 1). GFED2 used the estimates *by Andreae and Merlet* [2001] for inventorying global emissions of several gases [*van der Werf et al.*, 2006]. Ratios of C to CO emitted by global biomass burning according to GFED2 are plotted in Figure 11, and have an overall average of 5.8 ± 0.6. These monthly values were used to translate CO emissions to total C emissions. Semi-annual and annual values of CO and C emission anomalies are presented in Table 3 and Table 4.

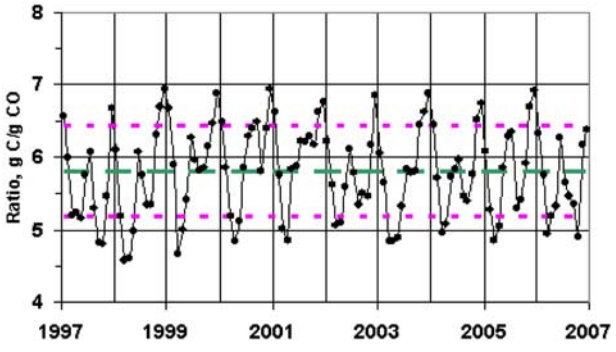

Figure 11. Ratios of total carbon to carbon monoxide monthly amounts emitted by wild biomass burning for global inventory by *van der Werf et al.* [2006]. Horizontal thick dash lines are mean and plus/minus standard deviation.

Table 3. Global Anomalies of CO Emissions Referred to 03/2000–02/2002[a]

	MOPITT, Jan–Jun	GFED, Jan–Jun	MOPITT, Jul–Dec	GFED, Jul–Dec	MOPITT, year	GFED, year
1997		−11.1		211.8		200.8
1998		132.9		102.1		235.0
1999		5.1		31.4		36.4
2000	−2.550	−8.6	48.8	−10.2	46.2	−18.8
2001	1.3393	−0.7	−47.228	10.2	−45.9	9.5
2002	−88.620	−5.3	96.4	67.8	7.8	62.5
2003	16.348	48.5	29.7	−6.8	46.0	41.7
2004	−42.010	0.4	91.4	48.6	49.4	49.1
2005	16.258	1.0	120.0	54.6	136.2	55.6
2006	−3.990	−45.6	187.6	82.2	183.6	36.5

[a]Total emission is estimated from MOPITT data and calculated for biomass burning (GFED2), in Tg for a specified period.

[47] Most of the discrepancy between GFED2 and MOPITT carbon estimates originates from the CO discrepancy. However, C/CO ratio introduces an additional uncertainty. How much extra CO in 2006 came from peat burning, for example? If we assume that 1/2 of CO was emitted by extratropical forests (Siberia and Canada) and the rest was emitted by peat fires (see Table 1), then the ratio C/CO would be 3.2, and instead of 1048 Tg C for the second half of 2006 (Table 3) the C emission anomaly would be only 578 Tg. Unfortunately, the degree of involvement of peat in the process of burning is difficult to quantify [*Kasischke et al.*, 2005] and requires further study.

5. Conclusions

[48] 1. The MOPITT CO total column data (version 3) from early 2000 until late 2006 were validated using two ground-based Sun-viewing spectrometers in Russia and Australia. The quality of the CO satellite total column

Table 4. Global Anomalies of Total C Emissions Referred to Period 03/2000–02/2002 Estimated From MOPITT CO Data and Calculated Using the GFED2 Model[a]

	MOPITT, Jan–Jun	GFED, Jan–Jun	MOPITT, Jul–Dec	GFED, Jul–Dec	MOPITT, year	GFED, year
1997		−31.9		869.9		838.0
1998		573.4		456.9		1030.3
1999		−0.9		134.5		133.6
2000	−10.4	−53.3	311.7	−59.2	301.3	−112.5
2001	18.5	14.1	−301.1	59.2	−282.6	73.3
2002	−479.3	−22.1	503.1	257.2	23.8	235.0
2003	88.6	196.1	160.3	−96.1	248.8	100.0
2004	−246.0	0.9	524.3	168.3	278.3	169.1
2005	87.4	−0.7	695.4	216.9	782.8	216.2
2006	−12.8	−252.6	1048.5	297.6	1035.7	45.1

[a]Emissions are measured in Tg. The C/CO ratios are plotted in Figure 11.

measurements can be assessed in terms of a proposed quality parameter that is calculated by averaging the standard *Profile Percent A priori* values over the tropospheric part of CO profile. Data with TCQP <60% have a precision better than ±13%. This estimate can be lowered if exact matching of two instruments could be achieved. This conclusion corroborates results of other validation experiments [*Emmons et al.*, 2004, 2007] for more favorable conditions, including a better matching.

[49] 2. In winter, the accuracy of MOPITT total column data for continental snow covered areas drops due to insensitivity to the boundary layer, especially during the night. Summer nighttime data are less accurate then daytime data, as well. Although there were no ground-truth stations in the tropics, quality parameters around ∼30% imply a sufficiently high accuracy.

[50] 3. Version 4 of AIRS CO total column measurements was compared to MOPITT data and to ground truth measurements. In many cases, especially in the NH, the AIRS data did not differ much from the other two data sets. A 20–40% positive bias was found in southeast Australia (FTIR) and in the tropics (MOPITT). This version of AIRS can be used only for qualitative analysis. The next version 5 is now in a process of release and is expected to be more precise.

[51] 4. Satellite instruments have an unparalleled ability for accurate monitoring of the global burden of carbon monoxide. However, permanent comparisons with ground truth data are necessary. For example, according to this validation experiment based on two stations, the MOPITT error for matching days has an upward drift (from underestimation to overestimation) of ∼1% per year. Further validation efforts are necessary to confirm this.

[52] 5. The positive trend of CO burden between 70°S and 70°N during the second half of the year amounted to +7.5 Tg a^{-1} or 1.9% a^{-1} and $R^2 = 0.74$. During the first half of the year no significant trend was observed (+1.5 Tg a^{-1} and $R^2 = 0.08$). This trend can only be partly explained by the above mentioned instrumental drift and probably reflects a growth of CO total emissions between 2000 and 2006.

[53] 6. Monthly changes of the burden anomaly can be converted into monthly mean anomalies of the source with the assumption of uniform [OH] sink with global distribution of [OH] from *Spivakovsky et al.* [2000]. These values were compared with anomalies of biomass burning emissions independently calculated from MODIS burned areas, NDVI from AVHRR, available emission factors and other data [*van der Werf et al.*, 2006]. A good correlation in timing and magnitudes indicates biomass burning as the main source of the CO emission IAV.

[54] 7. In 2006, the global annual emission anomaly amounted to (184 ± 40) Tg CO a^{-1} and 0.6–1.0 Pg C a^{-1} (assuming the ratios C/CO as 3.2 and 5.8 for lower and upper limits) in comparison with low-emission 2000 and 2001. Almost all amounts were emitted during second half of 2006. The box model used in this paper does not allow one to estimate contributions of various areas quantitatively. However, total columns measured by MOPITT indicate that two areas were the most important contributors in 2006: Indonesia and northern boreal fires mainly in Siberia.

[55] 8. Top-down estimates for CO and C are higher than the bottom-up calculations of biomass burning emissions in GFED2; in many cases the difference is a factor of 2 or up to 150 Tg CO/a. This disagreement can potentially be resolved if CO from variable sources, other than biomass burning, would be added to pyrogenic CO. Variations of biogenic NMHC look as promising to improve the agreement, but the magnitude and seasonal shapes of these variations are still uncertain. However, the MOPITT instrumental drift may explain this difference as well.

[56] 9. According to AR4 [*Solomon et al.*, 2007], all continents together are responsible for 0.9 ± 0.6 Pg C a^{-1} net sink for atmospheric carbon. Burning of continental biomass in 1997–1998 and in 2006 could convert the continents from a net sink to neutral area or even a weak source of carbon for the atmosphere. A monitoring of this emission using satellite CO measurements is important not only for CO itself but also for diagnosis and prognosis of the global CO_2 and CH_4 tropospheric burdens and biomass burning emissions.

[57] **Acknowledgments.** The work was supported by the NOAA grant NA04AOAR4310095 and NASA grants NAG5–11653–4, NNG046N426 for L. Yurganov and W. McMillan. E. Grechko, and A. Dzhola thank the Russian Fund for Basic Research (grant 05–05–64311) and the International Science and Technology Center (grant 3032) for a support. The authors are grateful to members of the MOPITT Science Team and, personally, to Merritt Deeter for useful clarifications. We thank also James Randerson for a helpful discussion and suggestions. Glen Engel-Cox kindly agreed to edit grammar and style.

References

Andreae, M. O., and P. Merlet (2001), Emissions of trace gases and aerosols from biomass burning, *Global Biogeochem. Cycles*, *15*, 955–966, doi:10.1029/2000GB001382.

Arino, O., and S. Plummer (Eds.) (2001), *Along Track Scanning Radiometer World Fire Atlas: Validation of the 1997–98 Active Fire Product*, ESA-ESRIN, Italy.

Aumann, H. H., et al. (2003), AIRS/AMSU/HSB on the Aqua mission: Design, science objectives, data products, and processing systems, *IEEE Trans. Geosci. Remote Sens.*, *41*, 253–264, doi:10.1109/TGRS.2002.808356.

Bergamaschi, P., R. Hein, M. Heimann, and P. J. Crutzen (2000), Inverse modeling of the global CO cycle: 1. Inversion of CO mixing ratios, *J. Geophys. Res.*, *105*(D2), 1909 doi:10.1029/1999JD900818.

Buchwitz, M., et al. (2005a), Atmospheric methane and carbon dioxide from SCIAMACHY satellite data: Initial comparison with global models of chemistry and transport, *Atmos. Chem. Phys.*, *5*, 941–962.

Buchwitz, M., R. de Beek, S. Noel, J. P. Burrows, H. Bovensmann, H. Bremer, P. Bergamaschi, S. Körner, and M. Heimann (2005b), Carbon monoxide, methane and carbon dioxide columns retrieved from SCIAMACHY by WFM-DOAS: Year 2003 initial data set, *Atmos. Chem. Phys.*, *5*, 3313–3329.

Butler, T. M., P. J. Rayner, I. Simmonds, and M. G. Lawrence (2005), Simultaneous mass balance inverse modeling of methane and carbon monoxide, *J. Geophys. Res.*, *110*, D21310, doi:10.1029/2005JD006071.

Chahine, M., C. Barnet, E. T. Olsen, L. Chen, and E. Maddy (2005), On the determination of atmospheric minor gases by the method of vanishing partial derivatives with application to CO_2, *Geophys. Res. Lett.*, *32*, L22803, doi:10.1029/2005GL024165.

Chahine, M. T., et al. (2006), AIRS: Improving weather forecasting and providing new data on greenhouse gases, *Bull. Am. Meteorol. Soc.*, *87*, 911–926, doi:10.1175/BAMS-87-7-911.

Cox, P. M., R. A. Betts, C. D. Jones, S. A. Spall, and I. J. Totterdell (2000), Acceleration of global warming due to carbon cycle feedbacks in a coupled climate model, *Nature*, *408*, 184–187, doi:10.1038/35041539.

Crisp, D., et al. (2004), The orbiting carbon observatory (OCO) mission, *Adv. Space Sci.*, *34*, 700–709, doi:10.1016/j.asr.2003.08.062.

Damoah, R., N. Spichtinger, C. Forster, P. James, I. Mattis, U. Wandinger, S. Beirle, T. Wagner, and A. Stohl (2004), Around the world in 17 days - Hemispheric-scale transport of forest fire smoke from Russia in May 2003, *Atmos. Chem. Phys.*, *4*, 1311–1321.

Deeter, M. N., et al. (2003), Operational carbon monoxide retrieval algorithm and selected results for the MOPITT instrument, *J. Geophys. Res.*, *108*(D14), 4399, doi:10.1029/2002JD003186.

Deeter, M. N., L. K. Emmons, D. P. Edwards, J. C. Gille, and J. R. Drummond (2004), Vertical resolution and information content of CO profiles retrieved by MOPITT, *Geophys. Res. Lett.*, *31*, L15112, doi:10.1029/2004GL020235.

DeMore, W. B., S. P. Sander, D. M. Golden, R. F. Hampson, M. J. Kurylo, C. J. Howard, A. R. Ravishankara, C. E. Kolb, and M. J. Molina (1997), Chemical kinetics and photochemical data for use in stratospheric modeling, *JPL Publ.*, *97–4*, 52 pp.

Dianov-Klokov, V. I. (1984), Spectroscopic studies of gaseous pollutants in the atmosphere over large cities (in Russian), *Izv. Akad. Nauk., Ser. Fiz.*, *20*, 883–900.

Dianov-Klokov, V. I., and L. N. Yurganov (1981), A spectroscopic study of the global space-time distribution of atmospheric CO, *Tellus*, *33*, 262–273.

Drummond, J. R. (1992), Measurements of Pollution in the Troposphere (MOPITT), in *The Use of EOS for Studies of Atmospheric Physics*, edited by J. C. Gille and G. Visconti, pp. 77–101, North-Holland, New York.

Edwards, D. P., et al. (2004), Observations of carbon monoxide and aerosols from the Terra satellite: Northern Hemisphere variability, *J. Geophys. Res.*, *109*, D24202, doi:10.1029/2004JD004727.

Edwards, D. P., G. Pétron, P. C. Novelli, L. K. Emmons, J. C. Gille, and J. R. Drummond (2006), Southern Hemisphere carbon monoxide interannual variability observed by Terra/Measurement of Pollution in the Troposphere (MOPITT), *J. Geophys. Res.*, *111*, D16303, doi:10.1029/2006JD007079.

Emmons, L. K., et al. (2004), Validation of Measurements of Pollution in the Troposphere (MOPITT) CO retrievals with aircraft in situ profiles, *J. Geophys. Res.*, *109*, D03309, doi:10.1029/2003JD004101.

Emmons, L. K., G. G. Pfister, D. P. Edwards, J. C. Gille, G. Sachse, D. Blake, S. Wofsy, C. Gerbig, D. Matross, and P. Nédélec (2007), Measurements of Pollution in the Troposphere (MOPITT): Validation exercises during summer 2004 field campaigns over North America, *J. Geophys. Res.*, *112*, D12S02, doi:10.1029/2006JD007833.

Frankenberg, C., J. F. Meirink, P. Bergamaschi, A. P. H. Goede, M. Heimann, S. Körner, U. Platt, M. van Weele, and T. Wagner (2006), Satellite chartography of atmospheric methane from SCIAMACHY on board ENVISAT: Analysis of the years 2003 and 2004, *J. Geophys. Res.*, *111*, D07303, doi:10.1029/2005JD006235.

Hamazaki, T., Y. Kaneko, A. Kuze, and K. Kondo (2005), Fourier transform spectrometer for Greenhouse Gases Observing Satellite (GOSAT), in *Enabling Sensor and Platform Technologies for Space-Borne Remote Sensing*, edited by G. J. Komar, J. Wang, and T. Kimura, *Proc. SPIE Int. Soc. Opt. Eng.*, *5659*, 73–80.

Haskins, R., and L. Kaplan (1992), Remote sensing of trace gases using the Atmospheric InfraRed Sounder, in *IRS'92: Current Problems in Atmospheric Radiation: Proceedings of the International Radiation Symposium, Tallinn, Estonia, 3–8 August 1992*, edited by S. Keevallik and O. Karner, pp. 278–281, A. Deepak, Hampton, Va.

Kasischke, E. S., E. J. Hyer, P. C. Novelli, L. P. Bruhwiler, N. H. F. French, A. I. Sukhinin, J. H. Hewson, and B. J. Stocks (2005), Influences of boreal fire emissions on Northern Hemisphere atmospheric carbon and carbon monoxide, *Global Biogeochem. Cycles*, *19*, GB1012, doi:10.1029/2004GB002300.

Leung, F.-Y. T., J. A. Logan, R. Park, E. Hyer, E. Kasischke, D. Streets, and L. Yurganov (2007), Impacts of enhanced biomass burning in the boreal forests in 1998 on tropospheric chemistry and the sensitivity of model results to the injection height of emissions, *J. Geophys. Res.*, *112*, D10313, doi:10.1029/2006JD008132.

McKernan, E., L. N. Yurganov, B. T. Tolton, and J. R. Drummond (1999), MOPITT validation using ground-based IR spectroscopy, in *Optical Spectroscopic Techniques and Instrumentation for Atmospheric and Space Research III*, edited by A. M. Larar, *Proc. SPIE Int. Soc. Opt. Eng.*, *3756*, 486–491.

McMillan, W. W., C. Barnet, L. Strow, M. Chahine, M. McCourt, P. Novelli, S. Korontzi, E. Maddy, and S. Datta (2005), Daily global maps of carbon monoxide: First views from NASA Atmospheric Infrared Sounder, *Geophys. Res. Lett.*, *32*, L11801, doi:10.1029/2004GL021821.

Miller, C. E., et al. (2007), Precision requirements for space-based XCO2 data, *J. Geophys. Res.*, *112*, D10314, doi:10.1029/2006JD007659.

Minzner, R. A. (1977), The 1976 standard atmosphere and its relationship to earlier standards, *Rev. Geophys. Space Phys.*, *15*, 375–384, doi:10.1029/RG015i003p00375.

Novelli, P. C., K. A. Masarie, P. M. Lang, B. D. Hall, R. C. Myers, and J. W. Elkins (2003), Reanalysis of tropospheric CO trends: Effects of the 1997–1998 wildfires, *J. Geophys. Res.*, *108*(D15), 4464, doi:10.1029/2002JD003031.

Palmer, P. I., et al. (2006), Quantifying the seasonal and interannual variability of North American isoprene emissions using satellite observations of the formaldehyde column, *J. Geophys. Res.*, *111*, D12315, doi:10.1029/2005JD006689.

Paton-Walsh, C., N. B. Jones, S. R. Wilson, V. Haverd, A. Meier, D. W. T. Griffith, and C. P. Rinsland (2005), Measurements of trace gas emissions from Australian forest fires and correlations with coincident measurements of aerosol optical depth, *J. Geophys. Res.*, *110*, D24305, doi:10.1029/2005JD006202.

Pétron, G., C. Granier, B. Khattatov, V. Yudin, J. Lamarque, L. Emmons, J. Gille, and D. P. Edwards (2004), Monthly CO surface sources inventory based on the 2000–2001 MOPITT satellite data, *Geophys. Res. Lett.*, *31*, L21107, doi:10.1029/2004GL020560.

Pfister, G., P. G. Hess, L. K. Emmons, J.-F. Lamarque, C. Wiedinmyer, D. P. Edwards, G. Pétron, J. C. Gille, and G. W. Sachse (2005), Quantifying CO emissions from the 2004 Alaskan wildfires using MOPITT CO data, *Geophys. Res. Lett.*, *32*, L11809, doi:10.1029/2005GL022995.

Price, C. (1993), Global surface temperatures and the atmospheric electric circuit, *Geophys. Res. Lett.*, *20*, 1363–1366, doi:10.1029/93GL01774.

Randerson, J. T., et al. (2006), The impact of boreal forest fire on climate warming, *Science*, *314*, 1130–1132, doi:10.1126/science.1132075.

Reichle, H. G., Jr., et al. (1999), Space shuttle based global CO measurements during April and October 1994, MAPS instrument, data reduction, and data validation, *J. Geophys. Res.*, *104*(D17), 21,443–21,454, doi:10.1029/97JD03299.

Rinsland, C. P., et al. (1998), Northern and Southern Hemisphere ground-based infrared spectroscopic measurements of tropospheric carbon monoxide and ethane, *J. Geophys. Res.*, *103*, 28,197–28,217, doi:10.1029/98JD02515.

Rodgers, C. D. (2000), *Inverse Methods for Atmospheric Sounding: Theory and Practice*, 256 pp., World Sci, Hackensack, N. J.

Solomon, S., et al. (2007), Technical summary, in *Climate Change 2007: The Physical Science Basis. Contribution of Working Group I to the Fourth Assessment Report of the Intergovernmental Panel on Climate Change*, edited by S. Solomon et al., 91 pp., Cambridge Univ. Press, New York.

Spivakovsky, C. M., et al. (2000), Three-dimensional climatological distribution of tropospheric OH: Update and evaluation, *J. Geophys. Res.*, *105*, 8931–8980, doi:10.1029/1999JD901006.

Stohl, A., C. Forster, A. Frank, P. Seibert, and G. Wotawa (2005), Technical note: The Lagrangian particle dispersion model FLEX-PART version 6.2, *Atmos. Chem. Phys.*, *5*, 2461–2474.

Stohl, A., et al. (2007), Arctic smoke record high air pollution levels in the European Arctic due to agricultural fires in Eastern Europe, *Atmos. Chem. Phys.*, *7*, 511–534.

Susskind, J., C. D. Barnet, and J. M. Blaisdell (2003), Retrieval of atmospheric and surface parameters from AIRS/AMSU/HSB data in the presence of clouds, *IEEE Trans. Geosci. Remote Sens.*, *41*, 390–409, doi:10.1109/TGRS.2002.808236.

Tao, Z. N., and A. K. Jain (2005), Modeling of global biogenic emissions for key indirect greenhouse gases and their response to atmospheric CO2 increases and changes in land cover and climate, *J. Geophys. Res.*, *110*, D21309, doi:10.1029/2005JD005874.

van der Werf, G. R., J. T. Randerson, L. Giglio, G. J. Collatz, P. S. Kasibhatla, and A. F. Arellano Jr. (2006), Interannual variability in global biomass burning emissions from 1997 to 2004, *Atmos. Chem. Phys.*, *6*, 3423–3441.

Wang, J. S., M. B. McElroy, J. A. Logan, P. I. Palmer, W. L. Chameides, Y. Wang, and I. A. Megretskaia (2008), A quantitative assessment of uncertainties affecting estimates of global mean OH derived from methyl chloroform observations, *J. Geophys. Res.*, doi:10.1029/2007JD008496, in press.

Warner, J., M. M. Comer, C. D. Barnet, W. W. McMillan, W. Wolf, E. Maddy, and G. Sachse (2007), A comparison of satellite tropospheric carbon monoxide measurements from AIRS and MOPITT during INTEX-A, *J. Geophys. Res.*, *112*, D12S17, doi:10.1029/2006JD007925.

Williams, E. R. (1992), The Schumann resonance: A global tropical thermometer, *Science*, *256*, 1184–1187, doi:10.1126/science.256.5060.1184.

Williams, E. R. (1994), Global circuit response to seasonal variations in global surface air temperature, *Mon. Weather Rev.*, *122*, 1917–1929, doi:10.1175/1520-0493[1994]122<1917:GCRTSV>2.0.CO;2.

Xiong, X., C. Barnet, C. Sweeney, E. S. Maddy, X. Liu, L. Zhou, and M. D. Goldberg (2008), Characterization and validation of methane products from the Atmospheric Infrared Sounder (AIRS), *J. Geophys. Res.*, doi:10.1029/2007JG000500, in press.

Yurganov, L. N., E. I. Grechko, and A. V. Dzhola (1997), Variations of carbon monoxide density in the total atmospheric column over Russia between 1970 and 1995: Upward trend and disturbances, attributed to the

influence of volcanic aerosols and forest fires, *Geophys. Res. Lett.*, *24*, 1231–1234, doi:10.1029/97GL50990.

Yurganov, L. N., E. I. Grechko, and A. V. Dzhola (1999), Zvenigorod carbon monoxide total column time series: 27 yr of measurements, *Chemosphere Global Change Sci.*, *1*, 127–136, doi:10.1016/S1465-9972(99)00012-4.

Yurganov, L. N., E. I. Grechko, and A. V. Dzhola (2002), Long-term measurements of carbon monoxide over Russia using a spectrometer of medium resolution, *Recent Res. Dev. Geophys.*, *4*, 249–265.

Yurganov, L. N., et al. (2004), A quantitative assessment of the 1998 carbon monoxide emission anomaly in the northern hemisphere based on total column and surface concentration measurements, *J. Geophys. Res.*, *109*, D15305, doi:10.1029/2004JD004559.

Yurganov, L. N., et al. (2005), Increased Northern Hemispheric carbon monoxide burden in the troposphere in 2002 and 2003 detected from the ground and from space, *Atmos. Chem. Phys.*, *5*, 563–573.

A. V. Dzhola and E. I. Grechko, Obukhov Institute of Atmospheric Physics, Russian Academy of Sciences, Moscow, 109017, Russia.

N. B. Jones, Department of Chemistry, University of Wollongong, Wollongong, NSW 2522, Australia.

W. W. McMillan and L. N. Yurganov, Joint Center for Earth System Technology, University of Maryland, Baltimore County, 1000 Hilltop Circle, Baltimore, MD 21250, USA.

G. R. van der Werf, Department of Hydrology and Geo-Environmental Sciences, Vrije Universiteit, De Boelelaan 1105, NL-1081 HV, Amsterdam, Netherlands.